A&A 463, 663–669 (2007)
DOI: 10.1051/0004-6361:20065048

Astronomy & Astrophysics

Analysis of ISO SWS01 spectra of S stars⋆

X. H. Yang[1,2,3], P. Chen[1], J. Wang[1], and J. He[1]

[1] National Astronomical Observatories/Yunnan Observatory, Chinese Academy of Sciences, PO Box 110 Kunming, Yunnan Province 650011, PR China
e-mail: [yangxh;chenps;jcwang;jinhuahe]@ynao.ac.cn
[2] Department of Physics, Chongqing University, Chongqing 400044, PR China
[3] Graduate School of Chinese Academy of Sciences, Beijing 100049, PR China

Received 20 February 2006 / Accepted 20 October 2006

ABSTRACT

The Infrared Space Observatory (ISO) Short-Wavelength Spectrometer (SWS01) plays an important role in studying properties of S stars. We reduce and analyze the SWS01 spectra of 17 S stars, and identify the candidate carriers of molecular absorption features. The ISO Spectral Analysis Package (ISAP) developed by the LWS and SWS Instrument Teams and Data Centers is used to process and analyze the SWS01 spectra of 17 S stars. The ISO archives of 17 S stars are obtained from the ISO database. Of 17 S stars, two stars are extrinsic S stars, the others are intrinsic S stars. The 15 intrinsic S stars can be divided into three groups (6 stars for Group I, 7 stars for Group II, and 2 stars for Group III) according to their Infrared Astronomical Satellite (IRAS) low-resolution spectra (LRS) and dust mass-loss rate $\dot{M}_{\rm dust}$, where $\dot{M}_{\rm dust}$ increases from Group I to II and III gradually. 17 S stars show the following properties: 1. two extrinsic S stars and 15 intrinsic S stars among different groups have different infrared properties; 2. two extrinsic S stars and 6 intrinsic S stars in Group I have similar ISO SWS01 spectra and their continua can be approximately described by a single blackbody representing the stellar photosphere, while some intrinsic S stars in Group I have 60 μm infrared excess; 3. for intrinsic S stars in Groups I, II, and III, their continua peak shifts toward longer wavelength from Groups I to II to III; 4. S stars in Groups II and III show obvious dust emission features in which the ∼10 μm dust features seem to display two different shapes. Moreover, two S stars (IRAS 00192-2020 & IRAS 15492+4837) present the 13 μm feature; 5. molecules H_2O, CO, and CO_2 greatly affect the ISO SWS01 spectra of S stars. It is noted that the absorption features of molecules CS and HCN usually thought to exist only in C stars may appear in the S stars.

Key words. stars: AGB and post-AGB – stars: circumstellar matter – infrared: stars

1. Introduction

All stars with initial mass 1 to 8 $M_\odot$ on the main sequence finally evolve through two red-giant phases in the late stage of stellar evolution (Iben & Renzini 1983). The second red-giant phase is referred to as the Asymptotic Giant Branch (AGB) phase, in which the photospheric chemical abundances are changing because helium shell flashing occurs and the helium-burning products (primarily ^{12}C) and *s*-process elements (including the short-lived isotope technetium) are mixed into the outer envelope during the third dredge-up phase. With the increase of the C/O ratio from <1 to >1 in the photosphere, the AGB stars usually evolve along the sequence M−MS−S−SC−C, as is confirmed by observations (Wood 1985; Little-Marenin & Little 1988; Chen et al. 1990).

S stars are often thought to be an intermediate phase of AGB evolution between M and C stars in which the C/O ratio of stars changes from 0.6 (MS stars) (Smith & Lambert 1985) to 0.8 (S stars) (Smith & Lambert 1986) and 1.0 (SC stars) (Keenan & Boeshaar 1980; Dominy et al. 1986), and their spectra are characterized by the absorption bands of ZrO and LaO molecules in the photosphere. However, some researches found that some non-variable S stars without technetium (Tc) may be binaries (Jorissen & Mayor 1988, 1992), and suggested that there may be two categories of S stars defined by whether or not they contain the unstable element Tc (Iben & Renzini 1983). S stars with Tc (also called intrinsic S stars or Tc-rich S stars) following the evolution sequence M−S−C are actually in the AGB phase. S stars without Tc (also called extrinsic S stars or Tc-deficient S stars) are found in binary systems with white dwarf (WD) companions. The unusual chemistry is believed to be due to mass transfer from the WD progenitor.

For AGB stars, the mass loss plays an important role and their infrared spectra are mostly affected by the composition of dust grains and the optical thickness of the circumstellar dust envelopes (CDEs). Currently, intrinsic S stars are observed to have CDEs, however extrinsic S stars do not present CDEs (Jorissen et al. 1993), which is consistent with the current understanding that extrinsic S stars are not in the AGB phase. Since S stars have the C/O ratio of the transitional range from oxygen- to carbon-dominated molecules and dust materials, their chemical properties in atmospheres and CDEs are different from those of both M and C stars (Ferrarotti & Gail 2002) and the differences should be reflected in molecule and dust features on infrared range. Therefore, it is very necessary to study the infrared spectra of S stars. Little-Marenin & Little (1988) analyzed the IRAS LRS spectra of MS, S, and SC stars and found a progression of emission features caused by dust grains in the 8–22 μm region. Chen & Kwok (1993) assembled IRAS LRS spectra of 149 S stars (including 121 S stars, 19 MS stars, and

⋆ Based on observations with ISO, an ESA project with instruments funded by ESA Member States (especially the PI countries: France, Germany, The Netherlands, and the United Kingdom) with the participation of ISAS and NASA.

9 SC stars) and proposed a new classification scheme, considering both the photospheric and circumstellar spectral properties for AGB stars. In general, the IRAS LRS spectra of S stars show either a featureless dust continuum or a silicate emission feature, while a few stars show a weak SiC emission feature. On the other hand, Noguchi & Kobayashi (1993) obtained the low-resolution near-infrared (NIR) spectra of 26 S stars and found the 2.4 μm CO and 2.7 μm H_2O absorption features, and suggested that the strength of the H_2O absorption is probably correlated with the atmospheric C/O ratio and the NIR colors. These early studies were compromised by the low-resolution, narrow wavelength range of the observations. Using the superior resolution and broader wavelength range of ISO-SWS, we re-investigate the IR spectra of S stars. The analysis presented in this paper focuses on the S stars observed by ISO. In Sect. 2 we describe the choice of samples and primary data processing. In Sect. 3 we discuss the ISO SWS01 spectra and spectral features of samples, and a discussion of the consequences and conclusions follow in Sect. 4.

2. The ISO SWS01 observations of S stars

We use objects listed in General Catalogue of Galactic S stars (GCGSS) (Stephenson 1984) to query the ISO archive and find that 20 S stars have the ISO SWS01 spectra that cover the 2.38–45.2 μm wavelength ranges with the spectral resolutions of 1000 to 200 (depending on observation and wavelength), while only 17 have usable SWS01 spectra, and 3 others show very large errors on the SWS01 spectra. Of the 17 S stars, 15 stars are intrinsic S stars (Jorissen et al. 1993) or candidate intrinsic S stars (Yang et al. 2006). Of the two remaining stars, one is an extrinsic S star (Jorissen et al. 1993) and the other is a candidate extrinsic S star (Yang et al. 2006) (hereafter, the objects with known type and candidates are not distinguished).

The ISO Spectral Analysis Package (ISAP[1]) was used to process and analyze SWS01 spectra. Small memory effects can be ignored and the average of up and down scans can be directly made. To do the absolute flux calibration ("Lines" as put by ISAP) of the SWS01 spectrum in the different bands, we use band 1A (2.38–2.60 μm) as the flux reference to calibrate the flux in the other bands. A small overlapping region exists in each pair of neighboring bands of SWS01 spectra, but actually long wavelength spectra show a large discrepancy in the overlapping region, and this effect on the overlapping spectra can be ignored in the studied range of 2.38–25.0 μm. Therefore, we simply link the spectrum of two adjacent bands using the end flux of their effective wavelength range. The reduced results of 17 ISO SWS01 spectra in 2.38–25.0 μm bands (thin lines) are shown in Fig. 2 (Fig. 2 will be described in Sect. 3.1).

3. Discussion

3.1. The classification of 17 S stars

Of the 17 S stars, two are extrinsic S stars (IRAS 13372-7136 and IRAS 23070+0824) and the others are intrinsic S stars. The 15 intrinsic S stars can be divided into three groups according to their IRAS LRS classes and $\dot{M}_{\rm dust}$: for Group I, LRS classes are of S and F and $\dot{M}_{\rm dust}$ $\sim 10^{-11}$ $M_\odot$ yr^{-1}; for Group II, LRS classes are of E and F and $\dot{M}_{\rm dust}$ $\sim 10^{-9}$–10^{-10} $M_\odot$ yr^{-1}; for Group III, LRS class is of E and $\dot{M}_{\rm dust}$ $\sim 10^{-8}$ $M_\odot$ yr^{-1}. Usually, IRAS LRS spectra were classified into nine groups by eye, based on the emission and absorption features and the continuum shape (Kwok & Volk 1997). For LRS class S, the IRAS LRS spectra closely approximate the Rayleigh-Jeans tail of the stellar photospheric continuum. For LRS class F, the IRAS LRS spectra show a featureless continuum flatter than that expected of a stellar photosphere. For LRS class E, the IRAS LRS spectra show the 9.7 μm silicate dust feature (Volk et al. 1991; Kwok & Volk 1997). The detailed information of 17 S stars is summarized in Table 1 (see columns' description in the footnote). In Table 1, the IRAS 19486+3247 (in Group II) with $\dot{M}_{\rm dust} \simeq 0.7 \times 10^{-10}$ $M_\odot$ yr^{-1} seems to be classified into Group I because its $\dot{M}_{\rm dust}$ given in Col. (5) is comparable to that of Group I; nevertheless it is classified into Group II because it exhibits strong dust emission on its ISO SWS01 spectra (IRAS LRS class of E) and has the dust mass-loss rate comparable to that of IRAS 22196-4612 in Group II according to the data from Sahai & Liechti (1995). Therefore, the real $\dot{M}_{\rm dust}$ of IRAS 19486+3247 may not be $\sim 0.7 \times 10^{-10}$ $M_\odot$ yr^{-1}. Here we adopt the data from Groenewegen & de Jong (1998) because the majority of their sample coincides with that presented here. In the calculation of S star magnitudes, we have considered measurement errors and interstellar extinction correction. If the measured errors of 2MASS *JHK* magnitudes are larger than the interstellar extinction correction, the latter correction can be ignored, otherwise the *JHK* magnitudes must be dereddened (Yang et al. 2006). The IRAS fluxes are converted to magnitudes using 12, 25, and 60 μm bands zero-magnitude fluxes of 28.3, 6.73, and 1.19 Jy, respectively (IRAS *Explanatory Supplement* 1988). The IRAS flux densities are taken from Jorissen & Knapp (1998) because they reprocessed the raw IRAS data of all S stars in their sample to correctly handle the following effects: 1) the 60 μm flux density may in some cases be seriously contaminated by Galactic cirrus emission; 2) the IRAS flux density are not appropriate in the case of slightly extended or variable sources; 3) the detectors may saturate on very bright sources, i.e., those with flux densities in excess of 1000 Jy (Jorissen & Knapp 1998).

Two color–color diagrams ($H-[12]$)–($K-[12]$) and ([12] – [25])–([25] – [60]) for 17 S stars are shown in Fig. 1, where different symbols represent extrinsic S stars and intrinsic S stars in different groups, respectively. From color–color diagram ($H-[12]$)–($K-[12]$), it is known that extrinsic S stars and intrinsic S stars in three groups are separately located on a uniform line. However, the Group II source, IRAS 05374+3153, is located in the Group I region. This may be caused by the uncertainty of color index measurement and interstellar extinction correction. For example, the measuring errors of H and K magnitudes are 0.202 and 0.196, respectively, and larger than interstellar extinction correction. The presence of the separate distribution shown in the ($H-[12]$)–($K-[12]$) diagram reflects the influence of dust mass-loss rate on the infrared properties of S stars. An increase of dust mass-loss rate causes the increase of the $K-[12]$ index from extrinsic S stars to intrinsic ones in Group I, Group II, and Group III, which is consistent with the $K-[12]$ index being a tracer for the mass-loss rate, proposed by several authors (e.g., Habing 1996; Jorissen et al. 1998). Extrinsic S stars and intrinsic S stars in three groups also display different properties in the ([12] – [25])–([25] – [60]) diagram, where various regions (labeled I to VII) defined by van der Veen & Habing (1988) and two ellipses (pointed by "Group I" and "Group II", respectively) are plotted. According to the definition of the regions labeled I to VII, we can deduce the CDE properties of S stars. Two extrinsic S stars located in region I should only have

[1] The ISO Spectral Analysis Package (ISAP) is a joint development by the LWS and SWS Instrument Teams and Data Centers. Contributing institutes are CESR, IAS, IPAC, MPE, RAL, and SRON.

Table 1. The infrared data of 17 S stars.

Group	Objects	GCGSS	Name	$\dot{M}_{\rm dust}$ (10^{-10} $M_\odot$ yr^{-1})	LRS Group	Sp type	J mag	H mag	K mag	[12] mag	[25] mag	[60] mag
(1)	(2)	(3)	(4)	(5)	(6)	(7)	(8)	(9)	(10)	(11)	(12)	(13)
Tc(No)	13372–7136C	0826	LY Mus	0.06	S	S6,2	2.143	1.218	0.868	0.173	0.044	0.105
	23070+0824	1322	GZ Peg	0.04	S	M4IIIS	0.841	–0.078	–0.402	–1.190	–1.199	–1.074
	00192–2020	0008	T Cet	0.81	F	M5–6Se	0.496	–0.482	–0.808	–2.118	–2.710	–2.720
	03452+5301C	0082	WX Cam		F	S5,8	3.910	2.777	2.203	1.419	0.754	–0.762
	20026+3640	1188	AA Cyg	1.10	S	S6,3	2.066	1.050	0.625	–0.382	–0.902	–1.636
	22476+4047C	1308	RX Lac	0.62	S	S7.5,1e	1.337	0.357	–0.023	–1.376	–1.715	–2.338
	22521+1640	1315	HR Peg	0.06	S	S5,1	2.306	1.239	1.041	0.028	–0.093	–0.036
	23595-1457	1346	W Cet	0.32	F	S6,3e	3.332	2.397	2.047	0.835	0.598	0.531
	00213+3817	0009	R And	15.4	E	S5–7,4–5e	2.024	0.765	0.122	–2.686	–3.542	–3.366
	05374+3153	0149	No Aur	2.0	E	M2S	2.122	1.128	0.971	–0.512	–1.349	–1.559
	15492+4837	0903	ST Her	4.0	E	M6.5S	0.743	–0.137	–0.542	–2.152	–2.916	–2.896
II	19354+5005	1150	R Cyg	35.4	E	S6,6e	/	/	/	–1.448	–2.238	–2.529
	19486+3247	1165	χ Cyg	0.7	E	S7,1.5e	0.168	–1.101	–1.695	–4.082	–4.474	–4.449
	20120-4433C	1196	RZ Sgr	13.7	F	S4,4	2.648	1.741	1.362	–0.352	–1.449	–2.625
	22196-4612	1294	π^1 Gru	8.7	E	S5,7	–0.715	–1.882	–2.351	–3.837	–4.614	–4.681
III	01159+7220C	0028	S Cas	181.1	E	S4,6e	3.625	1.965	1.091	–2.711	–3.641	–3.509
	19126-0708C	1115	W Aql	223.3	E	S6,6e	1.534	0.238	–0.556	–4.234	–5.073	–5.118

Notes: Column (1) gives the Tc-deficient property of 2 extrinsic S stars and the classification of 15 intrinsic S stars defined in this paper; Cols. (2)–(4) are the IRAS name, the number in Stephenson's (1984) GCGSS, and the common name, respectively; The letter "C" after "IRAS" means that the object is an extrinsic or intrinsic S star candidate; Col. (5) gives the $\dot{M}_{\rm dust}$ of the objects derived from the data of Groenewegen & de Jong (1998); Cols. (6) and (7) lists the classifications of the IRAS LRS spectra (Kwok et al. 1997) and the spectral type (Keenan 1954; Keenan & Boeshaar 1980; Little-Marenin & Little 1988), respectively; Cols. (8) to (10) give the 2MASS *JHK* magnitudes (Yang et al. 2006), respectively; Cols. (11) to (13) give the IRAS 12, 25, and 60 μm magnitudes, respectively.

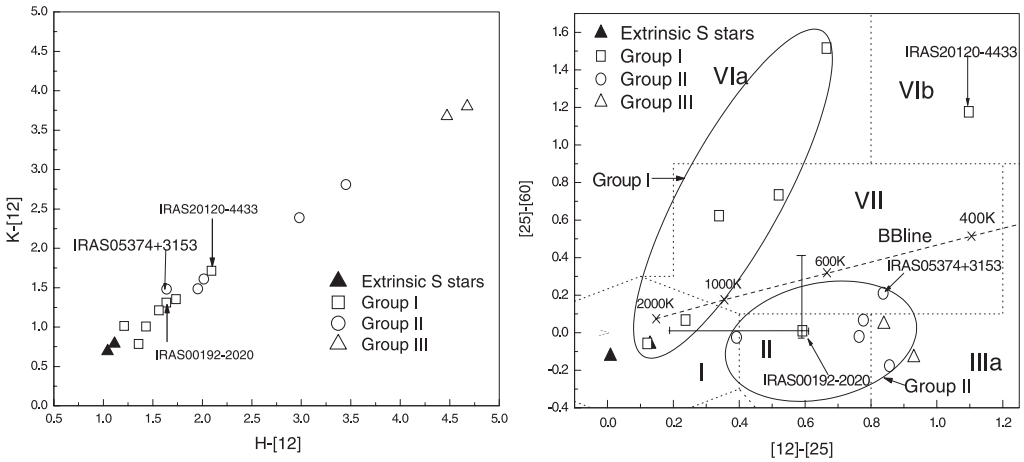

Fig. 1. The two color–color diagrams ($H-[12]$)–($K-[12]$) (*left*) and ([12] − [25])–([25] − [60]) (right) of 17 S stars. Different symbols represent extrinsic S stars (filled triangle), intrinsic S stars in Group I (open rectangle), in Group II (open circle), and in Group III (open triangle). The dashed line scaled with temperature in the ([12] − [25])–([25] − [60]) diagram shows a single blackbody line defined by van der Veen & Habing (1988).

photospheric IR colors without cool circumstellar shells. Two intrinsic S stars in Group III located in region IIIa should have thick circumstellar shells. The dispersed distribution of the intrinsic S stars in Groups I and II is described by two ellipses. The objects in Group I, except IRAS 00192-2020, should either have no dust shells or have detached cool dust shells. For IRAS 00192-2020, its unusual location is caused by the large uncertainty of the photometric data at 25 μm. For example, the photometric datum (81.66 Jy) from Jorissen & Knapp (1998) is more 25.86 Jy than that (55.8 Jy) from IRAS database. The objects in Group II, except IRAS 20120-4433, should have circumstellar shells whose optical depth varies amongst the Group II sources. For IRAS 20120-4433, its unusual location implies that it has relatively hot dust close to the star and relatively cool dust at large distances (van der Veen & Habing 1988).

3.2. Spectral properties

The ISO SWS01 spectra (thin lines) of 17 S stars in the wavelength range of 2.38–25.0 μm are shown in Fig. 2. The spectra in the 25.0–45.2 μm ranges are ignored due to higher noise. In Fig. 2, dashed lines are the single-blackbody spectra to fit the continua of ISO SWS01 spectra as a reference of near-infrared continua. This method was used to obtain the near-infrared blackbody temperatures of 29 C stars (Yang et al. 2004). Two ISO SWS01 spectra shown in the bottom right panel of Fig. 2 cannot be fitted by the single-blackbody spectra in the wavelength range of 2.38–7.0 μm, and their continua are not plotted.

From Fig. 2, it is generally seen that the same group of S stars has very similar ISO SWS01 spectra as expected because the classification of ISO SWS01 spectra in this paper is originally

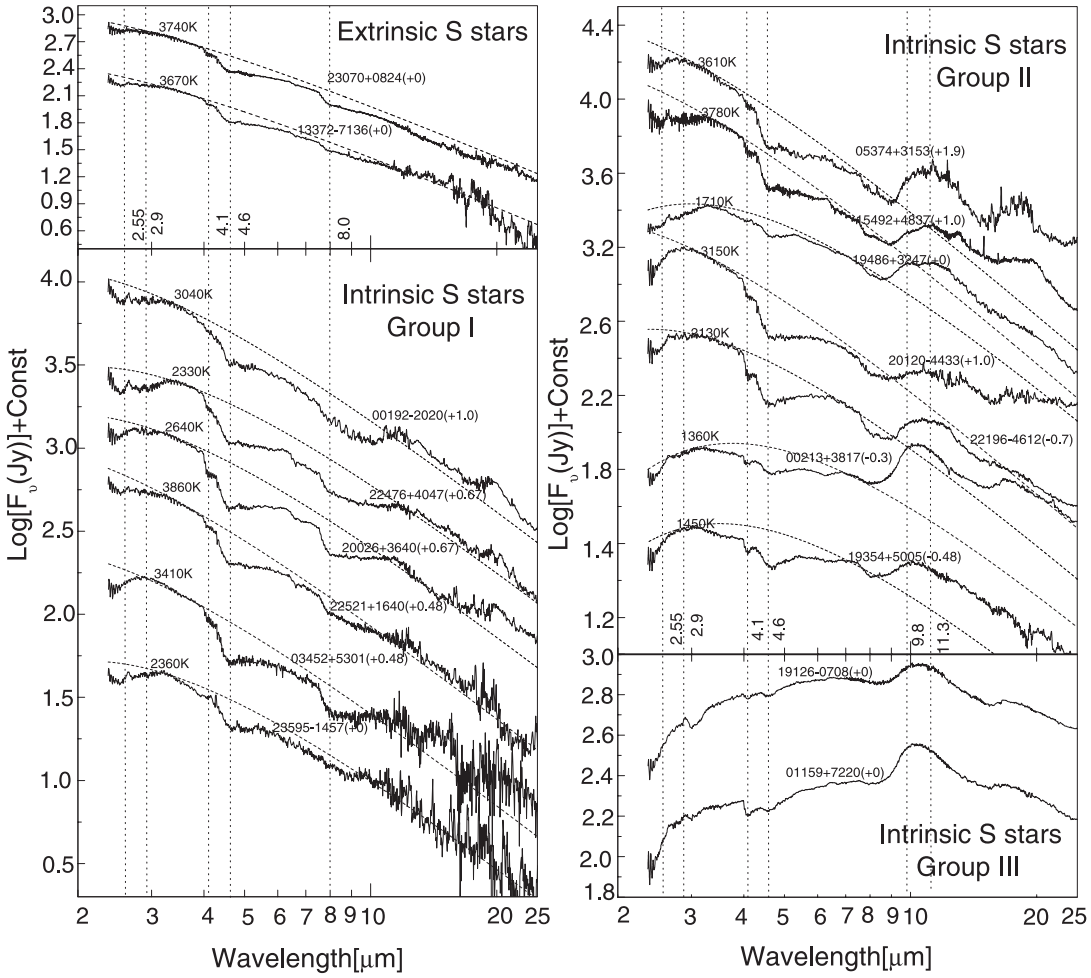

Fig. 2. ISO SWS01 Spectra (thin lines) are plotted in region of 2.38–25 μm for 2 extrinsic S stars (*left-top panel*), 6 intrinsic S stars (*left-bottom panel*) in Group I, 7 intrinsic S stars (*right-top panel*) in Group II, and 2 intrinsic S stars (*right-bottom panel*) in Group III. Dashed lines represent the single-blackbody spectra of 2 extrinsic S stars and 13 intrinsic S stars in Group I and II. Vertical dotted lines represent typical features on the spectra, and numbers on the right side of the dotted lines give their wavelengths in units of micrometers (the candidate carriers of these features will be given in the notes of Table 2). Labels (such as "00192-2020") above spectra are IRAS names of sources, and the number after IRAS names represents the value of Const. in the *Y* axis title.

based on IRAS LRS classes. Increasing dust mass-loss rates $\dot{M}_{\rm dust}$ lead to optical thickening of the circumstellar shell and thus the spectrum reddens. Consequently the $\dot{M}_{\rm dust}$ has a major affect on spectral dust features and can be used as a basis for classification of the spectra. Sloan & Price (1995, 1998) defined a sequence, labeled SE1−SE8, to describe the observed shapes of the silicate emission profile at 10 μm. Classes SE1−SE2, SE3−SE6, and SE7−SE8 show low-contrast alumina-rich dust emssion, structured silicate emission, and classic silicate emission, respectively (Sloan & Price 1995, 1998). Furthermore, Dijkstra et al. (2005) showed that, for Large Magellanic Cloud (LMC) stars, increasing mass-loss rates are correlated with a shift in the spectral features such that amorphous alumina gives way to increasing contributions from the classic 10 μm emission feature. On the other hand, the increase of $\dot{M}_{\rm dust}$ also changes ∼11 μm SiC emission features observed in carbon stars (Speck et al. 2005). Here, we will further discuss the ISO SWSO1 spectra of 17 S stars. For the two extrinsic S stars classified as S in IRAS classes, a single 2330–3860 K blackbody can well describe the continua of their spectra in the range of 2.4–25.0 μm, which represents the photosphere, and thus these stars do not have circumstellar dust shells. For the intrinsic stars in Group I, three stars (IRAS 00192-2020, IRAS 03452+5301, and IRAS 23595-1457) belong to *IRAS* LRS Class F and the others (IRAS 20026+3640, IRAS 22476+4047, and IRAS 22521+1640) belong to *IRAS* LRS Class S. Their spectra do not show the prominent 10 and 18 μm dust features, and the continua are also approximately described by a single blackbody of 2330–3860 K. Very low $\dot{M}_{\rm dust}$ precludes dust formation, and thus Group I stars also do not have much circumstellar dust. The ISO SWS01 spectra of Group I objects and two extrinsic S stars seem to be very similar and the similarity may be caused by the lower $\dot{M}_{\rm dust}$. In general, Group II stars that belong to IRAS LRS Class E (except IRAS 20120-4433), show obvious dust spectral features in the range of 9.0–25.0 μm and their continua peaks shift toward longer wavelengths compared to Group I stars. For two objects (IRAS 01159+7220 and IRAS 19126-0708) in Group III that belong to *IRAS* LRS class E, their SWS01 spectra show a red continuum whose peak is around 7 μm and are very different from that of Groups I and II. It indicates that a circumstellar shell caused by higher $\dot{M}_{\rm dust}$ has a lower color temperature than that of Group II. This case is similar to that seen in extreme carbon stars. The ISO SWS01 spectra of most of extreme carbon stars show an absorption feature around 10 μm, a stronger 30 μm emission, and a double-peaked spectral energy distribution (Volk et al. 2000), while the ISO SWS01 spectra of S stars

in Group III do not show the above features. The mass-loss rates of IRAS 01159+7220 (S Cas) and IRAS 19126-0708 (W Aql) in Group III are only 2.2×10^{-6} and 4.5×10^{-6} $M_{\odot}$ yr^{-1}, respectively (Jura 1988), and is much less than that of extreme carbon stars. Therefore the circumstellar shells around the two S stars are not thick enough to form self-absorption dust features.

3.3. Molecular absorption features

Main spectral features of 17 objects are listed in Table 2, where ones with the molecular absorption features are marked by letter "a", ones with the dust emission features are marked by letter "e", and ones with uncertain feature are marked by "?". In Table 2, some features are described with the wavelength appeared at the maximum or minimum of feature flux, others are described with the wavelength ranges between the red and blue end of the feature because these features have no uniform wavelength at the maximum or minimum of feature flux for all objects. From Table 2 and Fig. 2, some interesting information is obtained. 1) The stars in Group I and two extrinsic S stars have the same features on ISO SWS01 spectra in the 2.3–10.0 μm range. A special object (IRAS 03452+5301) seems not to show an absorption feature around 2.90 μm. For another object (IRAS 23595-1457), its spectra is not confirmed to have an absorption feature around 8.00 μm. 2) The objects in Groups I and II have similar spectral features in the 2.4–6.0 μm range. However they show different spectral features in the 6.0–25.0 μm range. For example, the objects of Group II do not show obvious absorption features at 8.0 μm shown in Fig. 2, and have obvious dust emission features peaking around 10.5 μm. 3) Two objects in Group III do not have a 2.65–3.20 μm absorption feature appearing in these of Groups I and II, but have a 2.9–3.30 μm absorption feature not appearing in these of Groups I and II.

Based on existing molecular data (Rothman 2003; Allard 2000; Goorvitch 1994), we preliminarily identify the candidate carriers of molecular absorption features shown in Fig. 1 and given in Table 2. Since H_2O absorption is usually seen in M stars, it is also important in determining the infrared spectral features of S stars (Woolf et al. 1964; Noguchi & Kobayashi 1993). The 2.36–2.65 μm spectral feature may be caused by an absorption of molecule H_2O+CO because H_2O and CO absorption cover the 2.36−2.66 μm range and the approximate 2.33−2.67 μm range, respectively. The 2.66−3.38 μm absorption may be from the molecules of H_2O+CO_2 because H_2O and CO_2 absorption cover the 2.65−3.40 μm range and the 2.65−2.97 μm range, respectively. However the 2.90−3.30 μm absorption shown on the spectra of Group III objects may be from molecule HCN covering the 2.9−3.25 μm range. The absorption around 4.1 μm may be from molecule CS covering the 3.86−4.35 μm range, but the presence of molecule CS in S stars with C/O < 1.0 seems not to be expected. The fairly broad 4.6 μm absorption may be from a mixture of the molecules of H_2O+CO+CO_2, because H_2O, CO, and CO_2 absorption cover 4.58−6.38 μm, 4.38−5.80 μm, and 4.16−4.57 μm ranges, respectively. The 8.0 μm absorption is from the molecule H_2O covering 6.38−9.7 μm range. The absorption features around 15 μm associated with molecular CO_2 are not found in the SWS01 spectra of 17 S stars. It was thought that S stars do not show obvious carbon-rich molecular absorption features, such as CS and HCN. However our identification results seem to show that some S stars have CS and HCN absorption features. Ferrarotti & Gail (2002) found that a dramatic change of gas composition occurs in the condensation zone of circumstellar shells with lower temperatures (e.g., $T < 1200$ K) at a critical carbon abundance of $\varepsilon_{\rm C,crit} = \varepsilon_{\rm O} - \varepsilon_{\rm Si} + \varepsilon_{\rm S}$ (=0.975$\varepsilon_{\rm O}$; here ε_x means the abundance of x element) (Ferrarotti & Gail 2002). When the carbon abundance is less than $\varepsilon_{\rm C,crit}$, the gas composition is almost dominated by O-rich molecules, while when the carbon abundance is more than $\varepsilon_{\rm C,crit}$ the gas composition is almost dominated by C-rich molecules. The gas composition does not change at $\varepsilon_{\rm C} = \varepsilon_{\rm C,crit}$ in the condensation zone with the temperature around 1600 K, but it does at the somewhat lower carbon abundance of $\varepsilon_{\rm C,crit} = \varepsilon_{\rm O} - \varepsilon_{\rm Si}$ (=0.948$\varepsilon_{\rm O}$) (Ferrarotti & Gail 2002) because the SiS molecule disappears above $T \approx 1600$ K. For the stellar photosphere with higher temperatures (around 2500 K) the transition between oxygen dominated and carbon dominated chemistry also occurs at $\varepsilon_{\rm C,crit} \approx \varepsilon_{\rm O} - \varepsilon_{\rm Si}$ (Ferrarotti & Gail 2002), but the change in the chemical composition is much slower in the stellar atmosphere than in the circumstellar condensation zone. The formation of carbon-dominated molecules such as HCN, CS, and CN can extend to a lower C/O ratio (=$\varepsilon_{\rm C}/\varepsilon_{\rm O}$), and the disappearance of oxygen-dominated molecules can extend to a higher C/O ratio than the case of circumstellar shells with lower temperatures. Therefore, the carbon-rich molecules such as HCN and CS may exist in the photosphere of S stars, and the 4.1 μm feature may be from molecule CS. However, it is not expected that HCN absorption features such as the 2.9−3.3 μm absorption feature appear in Group III objects because they have enough thick dust shells to dominate the flux density in the 2.4−7 μm ranges. A possible explanation is that such thick dust shells may also include a great number of HCN molecules because for the S stars when their circumstellar shells have the C/O ratio higher than the critical value ($\varepsilon_{\rm C,crit}/\varepsilon_{\rm O} = 0.975$), the abundant HCN molecule may form in the circumstellar shells with lower temperatures (Ferrarotti & Gail 2002). In the future, it is necessary to make the identification of the 4.1 μm absorption feature and the 2.9–3.3 μm absorption features in Group III objects.

3.4. Dust features

The 8.40−15.60 μm dust emission feature listed in Table 2 is not only different from the Silicate emission feature at 9.8 μm in the infrared spectra of M stars, but also different from the SiC emission feature at 11.3 μm in the infrared spectra of C stars. To show the dust feature of S stars, we plot the normalized 8.0−13.5 μm emission features in Group II and III in Fig. 3. Here, following the methodology of Speck et al. (2000), we assume that the stars' photosphere can be represented by a 3000 K blackbody. This blackbody was normalized to the ISO SWS01 spectrum at 8.0 μm and then subtracted from this observed spectrum. Speck et al. (2000) found that varying the blackbody temperature has very little effect on the normalized emission features.

Speck et al. (2000) studied the 10 μm dust features of 80 oxygen-rich AGB stars and 62 red supergiants and classified the dust features into six groups. For AGB stars, the six-group features are: 1) AGB broad features extending from 8 μm to 12.5 μm with little structure; 2) AGB broad features+silicate features consisting of a broad feature with an emerging 9.7 μm silicate bump; 3) four "classic" 9.7 μm silicate features becoming progressively narrower. For supergiants, the six-group features are: *featureless*, whose emission above the continuum is weak; *broad Super*, where the feature extends from ∼9 μm to ∼13 μm; and *four silicate Supers*, in which the "classic" 9.7 μm silicate feature also becomes narrower. From Fig. 3, we find that S stars in three panels also seem to have different dust features. The dust features in the top panel (hereafter, called "dust feature A") extend from 8.5−9 to 13.5 μm and peak longwards of 11 μm, while the dust features in the middle and bottom panels

Table 2. Main spectral features of 17 objects.

Group	Objects	Main spectral features Unit: μm
(1)	(2)	(3)
Tc-N	13372-7136	2.36–2.65a, 2.65−3.00a, 4.1a, 4.6a, 8.0a
	23070+0824	2.36–2.65a, 2.65−3.20a, 4.1a, 4.6a, 8.0a
	00192-2020	2.36−2.65a, 2.65−3.35a, 4.1a, 4.6a, 8.0a,13.0e, 13.88e, 14.97e, 16.19e, 19.8e,28.5e,31.5e
	03452+5301	2.36−2.88a, / , 4.10a, 4.60a, 8.0a
I	20026+3640	2.36−2.73a, 2.73−3.17a, 4.1a, 4.6a, 8.0a
	22476+4047	2.36−2.65a, 2.65−3.32a, 4.1a, 4.6a, 8.0a
	22521+1640	2.36−2.65a, 2.65−3.20a, 4.1a, 4.6a, 8.0a
	23595-1457	2.36−2.65a, 2.65−3.17a, 4.1a, 4.6a, 8.0a?
	00213+3817	2.36−2.63a?, 2.63−3.00a, 4.1a, 4.6a , 8.0−15.4e,15.3−21.0e
	05374+3153	2.36−2.65a?, 2.65−3.02a, 4.1a, 4.6a , 9.0−15.3e,15.30−19.7e
	15492+4837	2.36−2.65a, 2.65−3.25a, 4.1a, 4.6a , 8.85−15.6e,13.0e, 13.88e, 14.97e, 16.19e, 19.8e,28.5e,31.5e
II	19354+5005	2.36−2.88a, 2.88−3.02a, 4.1a, 4.6a , 8.0−15.0e,15.0−19.0e
	19486+3247	2.36−2.65a, 2.65−3.38a, 4.1a, 4.6a , 8.4−15.6e
	20120-4433	2.36−2.88a, 2.88−3.02a?, 4.1a, 4.6a , 8.9−15.4e?
	22196-4612	2.36−2.65a, 2.65−3.20a, 4.1a, 4.6a , 8.9−14.8e,14.6−21.0e
III	01159+7220	2.36−2.69a, 2.90−3.30a, 4.1a, 4.6a, 8.3−15.4e,15.4−22.5e
	19126-0708	2.36−2.65a, 2.90−3.30a, 4.1a, 4.6a, 8.3−15.4e,15.4−22.5e

The carrier of 2.36–2.65 μm absorption may be molecules H_2O+CO; the candidate carriers of 2.65–3.38 μm absorption may be molecules H_2O+CO_2; the candidate carrier of absorption around 4.1 μm may be molecule CS; the candidate carriers of 4.6 μm absorption from ∼4.2 to ∼6.4 μm may be molecules H_2O+CO+CO_2; the candidate carriers of 8.0 μm absorption may be molecules H_2O. However, the 2.90−3.30 μm absorption shown only on the spectra of Group III may be due to molecule HCN.

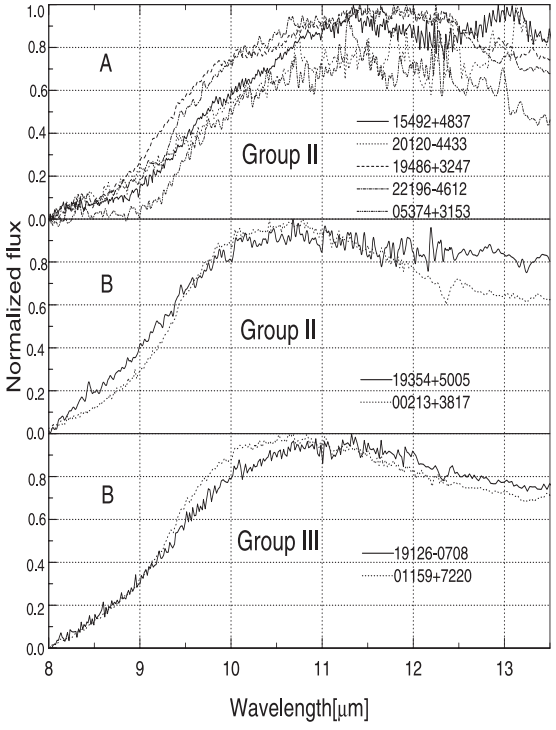

Fig. 3. Normalized 8.0−13.5 μm dust emission features (see text).

(hereafter, called "dust feature B") extend from 8.0 to 12.5 μm and peak around 10.5 μm. The dust feature A is similar to the supergiant broad feature defined by Speck et al. (2000), while the dust feature B is very similar to their AGB broad feature. The results from Speck et al. (2000) show that the AGB broad features can be well fit by a combination of magnesium silicate and amorphous alumina (Al_2O_3) and the supergiant broad features can be well fit by a combination of Ca-Al silicate and Al_2O_3. Therefore, for S stars, the dust feature A may be associated with Ca-Al silicate and Al_2O_3, and the dust feature B may be dominated by magnesium silicate and Al_2O_3. The spectra of two stars in Group III do not show much photospheric emission and thus the continuum cannot be represented by a 3000 K blackbody. For a Group III star, IRAS 01159+7220 (S Cas), a 550 K blackbody energy distribution was used to fit the continuum on its IRAS LRS spectra (Little-Marenin & Little 1988) and caused the blue and red ends of the dust feature to have nearly equal normalized flux (see Fig. 1 in Little-Marenin & Little's paper 1988). According to this result of Little-Marenin & Little (1988), the contribution from Al_2O_3 may be ignored, because Al_2O_3 emission can cause a rise at the red end of the normalized dust feature (see Fig. 19 in Speck et al.'s paper 2000). For another Group III star, IRAS 19126-0708 (W Aql), its dust feature in the wavelength range of 8–13.5 μm was observed and also classified as the AGB broad feature by Speck et al. (2000). We compare our extracted dust feature with the dust feature from Speck et al. (2000) and find that both features are consistent in general, which may be due to the fact that the same blackbody temperatures were employed to extract the dust features. While the shape of dust features in Group III objects, especially at its red end, is directly influenced by the confirmation of the continua, we find that the peak wavelength of dust features changes little and stands around 10.5 μm, which also suggests the contribution of Al_2O_3 to the dust features because the Al_2O_3 can result in the redward shift of peak wavelength of the 10 μm dust feature. It is interesting to note that none of the samples in this paper, either with high mass-loss rate or with low mass loss rate, display the pure silicate feature around 10 μm. Similarly, the conclusion from Sloan & Spice (1998) suggests that more

evolved stars with higher C/O ratios such as S stars should show Al_2O_3-dominated spectra, which is consistent with the lack of a "classic" ~10 μm silicate feature in our sample. However, our studied objects display two different types of dust features in the wavelength range 8–13.5 μm, e.g., the dust features A and B. Two types of dust features seem to be much more related by variable type and mass-loss rate than by spectral type given in Table 1. All objects displaying dust feature B are Mira variables and have higher mass-loss rates compared with the objects displaying dust feature A. In fact, the mass-loss rate dominates the density distribution of circustellar shells and therefore may cause S stars to display two different types of 8–13.5 μm dust features.

In addition to the above interesting dust features, we also pay attention to other important spectral information. In the objects studied here, only IRAS 00192-2020 (Group I) and IRAS 15492+4837 (Group II) are semi-regular variables and displays many emission features at 13.0, 13.88, 14.97, 19.8, 28.5, and 31.5 μm. IRAS 00192-2020 and IRAS 15493+4837 are belong to the F and E classes in term of IRAS LRS class, respectively, and do not exhibit 18 μm dust emission features. The 13.88 and 14.97 μm emission features are considered to be from warm carbon dioxide gas above the stellar photosphere (Justtanont et al. 1998). The warm CO_2 emission lines are associated with the unknown 13 μm feature (Justtanont at al. 1998; Sloan et al. 2003) and may provide a clue for the identification of carrier of 13 μm feature (e.g., Speck et al. 2000; Sloan et al. 2003). The 13 μm emission feature predominantly seen in the spectra of semi-regular variables (see Speck et al. 2000) is not ubiquitous amongst S stars, and is not followed by the 10 μm silicate feature for all the stars. The 10 μm silicate feature seems not to be seen on the ISO SWS01 spectra of IRAS 00192-2020, which suggests that the carrier of the 13 μm feature has formed around this star; nevertheless, silicate mineral does not exist or has no detectable abundance. At present, there are two candidate carriers for the 13 μm feature: Crystalline alumina (Al_2O_3, Glaccum 1995) and silica (SiO_2) grains (Speck et al. 1998, 2000). While other carriers have been proposed, they have been ruled out (see DePew et al. 2006 or Sloan et al. 2003, for details).

4. Summary and conclusion

In this paper, we have reduced and analyzed the ISO SWS01 spectra of 17 S stars (including 2 extrinsic S stars and 15 intrinsic S stars) and preliminarily identify the candidate carriers of molecular absorption features. The 15 intrinsic S stars can be divided into three groups according to their IRAS LRS classes and $\dot{M}_{\rm dust}$, which increases from Groups I to II and III gradually. 2 extrinsic S stars and 6 intrinsic S stars in Group I have similar ISO SWS01 spectra. They have lower $\dot{M}_{\rm dust}$ and cannot form an optical circumstellar shells. Some intrinsic S stars in Group I have 60 μm infrared excess, which is consistent with their low mass-loss rates. For 7 intrinsic S stars in Group II, their continua peak shifts toward longer wavelengths than the ones in Group I generally, and their SWS01 spectra show obvious dust emission features. For 2 intrinsic S stars in Group III, their SWS01 spectra show a red continuum peaking around 7 μm. Both the IRAS color–color diagram ([12] − [25])–([25] − [60]) and ISO SWS01 spectra indicate that these stars have a thick circumstellar shell caused by higher $\dot{M}_{\rm dust}$. The shell with low color temperatures is so thick that its emission dominates over the ISO SWS01 wavelength ranges.

Excluding those S stars with no or cool, detached CDEs, the S stars in our sample seem to exhibit two shapes of dust spectral feature in the 8–14 μm range. One type may be associated with a combination of Ca-Al silicate and amorphous alumina. Other type may be related with a combination of magnesium silicate and amorphous alumina. Two S stars, IRAS 00192-2020 and IRAS 15492+4837, have the 13 μm feature, while IRAS 00192-2020 does not have a 10 μm silicate feature. It implies that the 13 μm feature is not always followed by the 10 μm silicate feature. Molecules H_2O, CO, and CO_2 greatly influence the molecular absorption features of ISO SWS01 spectra for S stars. The 4.1 μm absorption feature and the 2.9–3.3 μm absorption feature appearing in Group III objects may be caused by molecules CS and HCN, respectively.

Acknowledgements. We are grateful to Dr. Speck for the suggests and comments on this paper. This work is supported by the National Natural Science Foundation of China under Grant Nos. 10503011 and 10433030.

References

Allard, F., Hauschildt, P. H., Schwenke, D. 2000, ApJ, 540, 1005
Chen, P. S., Gao, H., Bao, M. X., et al. 1990, in The Infrared Spectral Region of Stars, ed. C. Jaschek, & Y. Andrillat (Cambridge University Press), 385
Chen, P. S., Kwok S. 1993, ApJ, 416, 769
DePew, K., Speck, A., Dukstra, C. 2006, ApJ, 640, 971
Dijkstra, C., Speck, A. K., Reid, R. B. 2005, ApJ, 633, L133
Dominy, J. F., Wallerstein, G., & Suntzeff, N. B. 1986, ApJ, 300, 325
Ferrarotti, A. S., & Gail, H. P. 2002, A&A, 382, 256
Goorvitch, D. 1994, ApJS, 95, 535
Groenewegen, M. A. T., & de Jong, T. 1998, A&A, 337, 797
Glaccum, W. 1995, in Airborne Astronomy Symp. on the Galactic Ecosystem: From Gas to Stars to Dust, ed. M. R. Hass, J. A. Davidson, & E. F. Erickson (San Francisco: ASP), ASP Conf. Ser., 73, 395
Habing, H. J. 1996, A&AR, 7, 97
Iben, I. J., Renzini A. 1983, ARA&A, 21, 271
IRAS Explanatory Supplement, Second Edition 1988, Joint IRAS Science Working Group, Washington DC, US GPO
Jorissen, A., & Mayor, M. 1988, A&A, 198, 187
Jorissen, A., & Mayor, M. 1992, A&A, 260, 115
Jorissen, A., & Frayer, D. T., Johnson, H. R., et al. 1993, A&A, 271, 463
Jorissen, A., & Knapp, G. R. 1998, A&AS, 129, 363
Justtanont, K., Feuchtgruber, H., de Jong, T., et al. 1998, A&A, 330, L17
Jura, M. 1988, ApJS, 66, 33
Keenan, P. C. 1954, ApJ, 120, 484
Keenan, P. C., & Boeshaar, P. C. 1980, ApJS, 43, 379
Kwok, S., & Volk, K. 1997, ApJS, 112, 557
Little-Marenin, I. R., & Little, S. J., 1988, ApJ, 333, 305
Noguchi, K., & Kobayashi, Y. 1993, PASJ, 45, 85
Rothman, L. S., Barbe, A., Chris Benner, D., et al., 2003, JQSRT, 82, 5
Sahai, R., Liechti, S. 1995, A&A, 293, 198
Sloan, G. C., Price, S. D. 1995, ApJ, 451, 758
Sloan, G. C., Price, S. D. 1998, ApJS, 119, 141
Sloan, G. C., Kraemer, K. E., Goebel, J. H., et al. 2003, ApJ, 594, 483
Sloan, G. C., Kraemer, K. E., Matsuura, M., et al. 2006, [arXiv:astro-ph/0603607]
Smith, V. V., & Lambert, D. L. 1985, ApJ, 273, 742
Smith, V. V., & Lambert, D. L. 1986, ApJ, 311, 843
Speck, A. K., 1998, Ph.D. Thesis, Univ. College London
Speck, A. K., Barlow, M. J., Sylvester, R. J., et al. 2000, A&AS, 146, 437
Speck, A. K., Thompson, G. D., Hofmeister, A. M. 2005, ApJ, 634, 426
Stephenson, C. B. 1984, General Catalogue of Galactic S stars. (Warner, & Swasey Obs.), 3, 1 (GCGSS)
Tielens, A. G. G. M. 1990, in From Miras to Planetary Nebulae: Which Path for Stellar Evolution?, ed. M. O. Mennessier, & A. Omont (Gif-sur-Yvette: Éditions Frontières), 186
van der Veen, W. E. E. J., Habing, H. J. 1988, A&A, 194, 125
Volk, K., Kwok, S., Stencel, R., et al. 1991, ApJS, 77, 607
Volk, K., Xiong, G. Z., Kwok, S. 2000, ApJ, 530, 408
Wood, P. R. 1985, in CoolS stars with Excesses of Heavy Elements, eds. M. Jaschek, & P. C. Keenan (Reidel), 357
Woolf, N. J., Schwarzschild, M., & Rose, W. K. 1964, ApJ, 140, 833
Yang, X. H., Chen, P. S., He, J. H. 2004, A&A, 414, 1049
Yang, X. H., Chen, P. S., Wang, J. C., et al. 2006, AJ, 132, 1468